

## Phase Behavior and Spontaneous Vesicle Formation in Aqueous Solutions of Anionic Ammonium Dodecyl Sulfate and Cationic Octadecyl Trimethyl Ammonium Chloride Surfactants

Kye-Hong Kang, Hong-Un Kim,<sup>a</sup> and Kyung-Hee Lim\*

Department of Chemical Engineering, Chung-Ang University, Seoul 156-756, Korea. \*E-mail: khlim@cau.ac.kr

Received February 8, 2007

Phase behavior for the mixed aqueous surfactant systems of cationic octadecyl trimethyl ammonium chloride (OTAC)/anionic ammonium dodecyl sulfate (ADS)/water was examined. Below the total surfactant concentrations of 1.5 m molal, mixed micelles were formed. At the total surfactant concentrations higher than 1.5 m molal, there appeared a region where mixed micelles and vesicles coexist. As the surfactant concentration increased, the systems looked very turbid and much more vesicles were observed. The vesicles were spontaneously formed in this system and their existence was observed by negative-staining transmission electron microscopy (TEM), small-angle neutron scattering (SANS) and encapsulation efficiency of dye. The vesicle region was where the molar fraction  $\alpha$  of ADS to the total mixed surfactant was from 0.1 to 0.7 and the total surfactant concentration was above  $5 \times 10^{-4}$  molality. The size and structure of the vesicles were determined from the TEM microphotographs and the SANS data. Their diameter ranged from 450 nm to 120  $\mu$ m and decreased with increasing total surfactant concentration. The lamellar thickness also decreased from 15 nm to 5 nm with increasing surfactant concentration and this may be responsible for the decrease in vesicle size with the surfactant concentration. The stability of vesicles was examined by UV spectroscopy and zeta potentiometry. The vesicles displayed long-term stability, as UV absorbance spectra remained unchanged over two months. The zeta potentials of the vesicles were large in magnitude (40-70 mV) and the observed long-term stability of the vesicles may be attributed to such high  $\zeta$  potentials.

**Key Words :** Phase behavior, Cationic-anionic system, Vesicle, Zeta potential, SANS

### Introduction

The surfactants used in industrial products, processes, and practical applications almost consist of a mixture of surfactants. Mixed systems are less expensive than isomerically pure surfactants and they often provide better performances which arise from the deliberate formulation of mixtures of different surfactant types to exploit synergistic behavior. Hence, it is essential to understanding how surfactants interact in mixtures.<sup>1</sup>

In solutions containing two or more surfactants, the tendency of aggregated structures formed is substantially different from that in solutions consisting of only pure surfactant. Such different tendency results in dramatic changes in properties and behavior of mixed surfactant solutions.<sup>2</sup> Especially, mixing two surfactant ions of opposite charges, cationic/anionic (catanionic) surfactant mixtures show remarkably different physicochemical properties and behavior such as reductions in critical micelle concentration and surface tension.<sup>3,4</sup>

Vesicles can be formed spontaneously for various mixed surfactants systems. These vesicles have a limited solubility in water and a low permeability. However, once they are formed, they remain as vesicles for a long time due to their excellent stability. Since vesicles contain the continuous

phase in their core and their sizes can be of 30-100 nm, they can be used as microcapsules and also as capsules for agents in assays and drug delivery, microreactors for artificial photosynthesis, and substrates for a variety of enzymes and proteins.<sup>5</sup> As for the drug delivery vehicles, catanionic vesicles are as effective as niosomes which are derived from aqueous nonionic surfactant solutions, and more stable than liposomes.<sup>6</sup> Recently, vesicles have also provided compartments for preparation of nanoparticles.<sup>7-9</sup>

There have been observations of spontaneously formed vesicles in mixtures of surfactants: to name a few of them, for catanionic systems with single alkyl chains cetyltrimethylammonium tosylate (CTAT)/sodium dodecylbenzene sulfonate (SDBS),<sup>5,10,11</sup> dodecyltrimethylammonium chloride (DTAB)/sodium dodecyl sulfate (SDS),<sup>12,13</sup> cetyltrimethylammonium bromide (CTAB)/sodium petyl sulfate (SPS),<sup>14</sup> CTAB/SOS (sodium octyl sulfate),<sup>14,15</sup> and CTAB/SPDS (sodium pentadecyl sulfate)<sup>14</sup> and for mixtures of cationic surfactant with double alkyl chain and anionic surfactant with single alkyl chain didodecyltrimethylammonium bromide (DDAB)/SDS<sup>16</sup> and DDAB/sodium decyl sulfate (SDeS)<sup>17</sup> have been examined.

Cationics have been known to exhibit excellent antistatic effects and softness. Hydrocarbons higher than are normally employed in cosmetics and toiletries<sup>18,19</sup> and octadecyl trimethyl ammonium chloride (OTAC) is probably the most commonly used in these applications. As for anionics, SDS

<sup>a</sup>Present address: Hyosung R&D Center, Gyeonggi 431-080, Korea

is the most well-known, and widely used in industry, and plus it has been extensively studied in relation for its micellization, properties, and phase behavior.<sup>20,21</sup> However, in acidic solutions or at high temperatures, SDS undergoes autocatalytic acid hydrolysis, and dodecanol and sodium hydrogen sulfate are produced.<sup>22,24</sup> These products are believed to cause skin irritation.<sup>21</sup> In contrast, ammonium dodecyl sulfate (ADS) is less hydrolyzed in acidic solutions<sup>25</sup> and less skin-irritant than SDS.<sup>21,22</sup>

For these reasons, the use of ADS and OTAC in the cosmetic and toiletry industry has been expanding<sup>26,27</sup> and this is why the mixed systems of these surfactants were chosen. Previously mixed micellization of ADS/OTAC aqueous solutions were reported.<sup>28</sup> In this article, we report the phase behavior and spontaneous vesicle formation of this mixture. The phase behavior of the ADS/OTAC mixed system was examined by visual inspection, electrical conductometry, surface tensiometry, transmission electron microscopy (TEM), and small-angle neutron scattering (SANS). Also, the size, structure, and stability of spontaneously formed ADS/OTAC vesicles were examined by TEM, encapsulation efficiency of dye, SANS, UV absorbance spectroscopy, and zeta potentiometry.

## Experimental

**Materials.** The cationic surfactant octadecyltrimethyl ammonium chloride (OTAC) and anionic surfactant ammonium dodecyl sulfate (ADS) were purchased from Fluka. OTAC had a stated purity of 98% and ADS was in a form of 30% aqueous solution. For further purification the surfactants were first placed in a rotary evaporator to reduce the water and volatile material content. Then, OTAC was recrystallized twice from absolute ethanol. ADS was also recrystallized first from 90% ethanol and then twice from absolute ethanol. The purified surfactants were finally dried in an evacuated desiccator.<sup>29</sup> Water was distilled and deionized. For the formation of vesicles, ADS and OTAC at various molar ratios and total concentrations were weighed, delivered to water, and then mixed thoroughly through magnetic stirring.

**Electrical Conductivity Measurements.** The critical micelle concentrations (CMC's) were determined by electrical conductometry and interfacial tensiometry. For the conductivity measurements of surfactant solutions, a Radiometer (Paris, France) Model CDM 210 conductivity meter and a Model CDC641T conductivity cell with platinized electrodes were used. Platinized platinum electrodes were chosen to improve the accuracy of the conductivities by reducing any electrode polarization effects. The conductivity cell was calibrated with standard KCl solutions and its cell constant was determined to be  $0.7443 \text{ cm}^{-1}$ . The surfactant concentrations were changed by additions of deionized water from a burette to the surfactant solution, which was contained in a jacketed, thermostatic beaker. The surfactant solution was mixed thoroughly by magnetically driven stirring. The temperature was controlled within  $0.1 \text{ }^\circ\text{C}$  by a thermostat bath (Model VS-1205WP-CWO, Vision Scientific, Seoul,

Korea).

**Surface Tension Measurements.** The surface tensions of surfactant solutions were measured with a du Noüy KSV (Helsinki, Finland) Model Sigma70 and Cahn (DCA-315, USA) tensiometers using a platinum ring. The surfactant solutions were added by a microsyringe to water in a thermostatted glass vessel, and the surface tension was measured after thorough mixing with a magnetic stirrer. The temperature of the surfactant solutions was controlled within  $0.1 \text{ }^\circ\text{C}$  by a Jeio Tech (Seoul, Korea) Model VTRC-620 thermostat bath.

**Phase Behavior Study.** For the phase behavior of the ADS/OTAC/water system, samples of known compositions (wt %) were placed in a microprocessor-controlled thermostat with viewing windows (Vision Scientific, Seoul, Korea, Model VS-1205WP-CWO) for several days. Then, phase separation was visually observed and the number of phases of each sample was recorded. The phase separation was assumed to be complete when there was no appreciable change in phase volumes. In each phase region subdivisions were made by measuring mixed CMCs with conductometry and tensiometry and observing vesicles with electron microscopy.

**Vesicle Observation by Negative-Staining Transmission Electron Microscopy (TEM).** Samples were negatively stained with 2% (w/w) uranyl acetate solution according to the previously reported procedures.<sup>30</sup> Vesicles were observed and their electron micrographs were taken by JEM 200CX (Tokyo, Japan).

**Zeta Potential Measurements by Photon Correlation Spectroscopy.** Zeta ( $\zeta$ ) potentials of vesicles were measured by ZetaSizer 2000 (Malvern Instruments Ltd.). The principle on which the measurements were based was the Doppler electrophoresis with light scattering. The samples of the vesicles of ADS/OTAC mixed surfactants were prepared at the total surfactant concentrations slightly above the phase boundary, so that the  $\zeta$  potential measurements were affected least by multiple scattering and so that noninvasive measurements were done without any dilution of the samples. Each sample was injected to the cell by the syringe and at this time care had to be taken of not producing bubbles in the cell. If the bubbles were produced in the cell, their movement would be seen as the movement of particles and would change the result. The viscosity of  $1.002 \text{ cP}$  and dielectric constant of  $80.4$  were used for the calculations, since the solvent used was de-ionized water and the very small amount of surfactants used would make presumably this values changed little.

**UV Absorbance Measurements.** UV absorbance was measured by UV/VIS spectrophotometer (V-550, Jasco) to examine vesicle stability and concentrations of the dye, bromophenol blue, encapsulated in the vesicles. The spectra of the dye had specific peak at  $590 \text{ nm}$ . From the magnitudes of the peak, the concentrations of bromophenol blue in the solutions were determined.

**Encapsulation of Vesicles.** Aqueous solutions of bromophenol blue ( $0.05\text{--}0.3 \text{ mM}$ ) were as used in place of water in

making vesicles. When vesicles were formed in the dye solutions, the vesicles should contain some portion of the dye bromophenol blue in their core. When this vesicular dispersion flows through the chromatography column packed with Sephadex G-25 gel (100-300  $\mu\text{m}$ , Aldrich), the other portion of the dye which was uncaught by the vesicles should be in the effluent solution flowing out of the column.<sup>31</sup> The concentration of the dye in the effluent solution was determined by UV absorbance and the encapsulation efficiency was calculated.

**Small-Angle Neutron Scattering (SANS).** This experiment was performed at the SANS facility of the Korea Atomic Energy Research Institute. The scattering vector  $q$  and neutron wavelength ranged from 0.006 to 0.6  $\text{\AA}^{-1}$  and 4 to 8  $\text{\AA}$ , respectively. Also, wavelength resolution was 10% with full width at half-maximum value. The samples were prepared in  $\text{D}_2\text{O}$  solution and kept in quartz cylindrical cells (Next Instrument Co.) with a path length of 2 mm and outside diameter of 22 mm. The calibration of absolute scattering intensity was carried out using silica samples. The scattering intensity was furthermore normalized with respect to that of  $\text{D}_2\text{O}$ .<sup>32</sup>

## Results and Discussion

**Phase Behavior.** The phase behavior of a mixture focuses on the examination of how many phases exist and what their compositions and structures are. Through this examination properties of the mixture can be better understood.<sup>33</sup>

At 40.5  $^\circ\text{C}$  the aqueous mixture of the catanionic system displayed the regions of single, two, three and four phases, as shown in Figure 1a. The two- and three-phase regions almost filled the triangular coordinates. The four-phase region appeared when ADS and water were rich and OTAC was poor, and the four phases consisted of opaque solid, opaque liquid, transparent crystal, and transparent liquid. As the temperature increased to 51.2  $^\circ\text{C}$ , the four-phase region disappeared and the three-phase region shrank. Instead, two-phase region expanded. This may arise from the fact that the solubility of the precipitates of ADS/OTAC increased with temperature.

At the higher temperature of 60.3  $^\circ\text{C}$  the two-phase region expanded further (Figure 1b). Around the composition of ADS/OTAC/water = 18/10/72 (wt% ratio), single phase was observed. This single-phase region was neighbored by the three-phase region as well as the two-phase region. Hence, it appears that this observation violated the so-called "alternation rule",<sup>33</sup> which states that an alternation between odd and even numbers of phases occurs (in increment of one) along isoplethal and isothermal process trajectories.

Phase behavior of very dilute aqueous mixtures of the anionic ADS and cationic OTAC was examined and the results are presented in a triangular coordinate in Figure 2a and in a rectangular coordinate Figure 2b. The concentration of each surfactant was less than 0.2 wt % and the total surfactant concentration was below 0.4 wt %. The phase diagram is characterized by four distinct phase regions<sup>28</sup> of

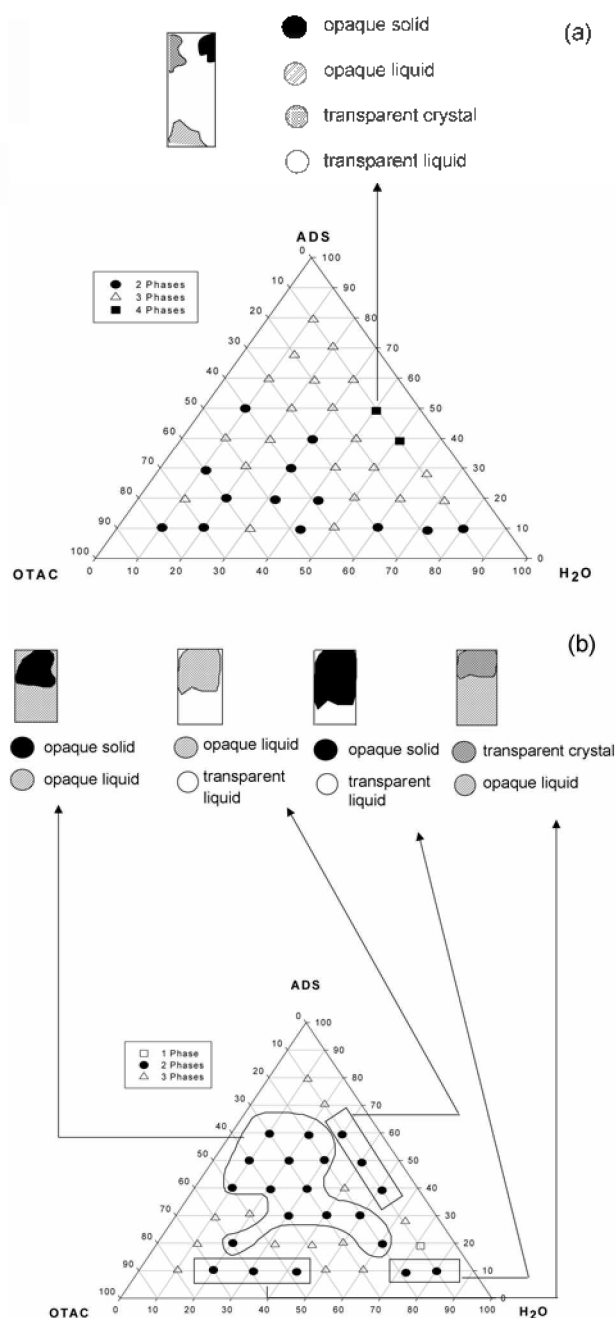


**Figure 1.** Overall phase diagram of ADS/OTAC/water system at (a) 40.5  $^\circ\text{C}$  and (b) 60.3  $^\circ\text{C}$ .

isotropic molecular solution (I), micellar solution (M), vesicles (V), and a mixture of micelles and vesicles (M+V).

The isotropic solution is clear and its region (I) is extended up to the pure component CMCs in aqueous solutions that are 0.392 m molal (0.0137 wt fraction) for OTAC and 6.258 m molal (0.1771 wt fraction) for ADS, respectively.<sup>34</sup> The isotropic solution region at the ADS-rich side is wider than that at the OTAC-rich side because of the disparity of CMC (CMC of ADS is about 20 times larger than that of OTAC). The OTAC-rich isotropic region is seen very small near the water apex in the triangular coordinate.

In the micellar region (M) mixed micelles of ADS and

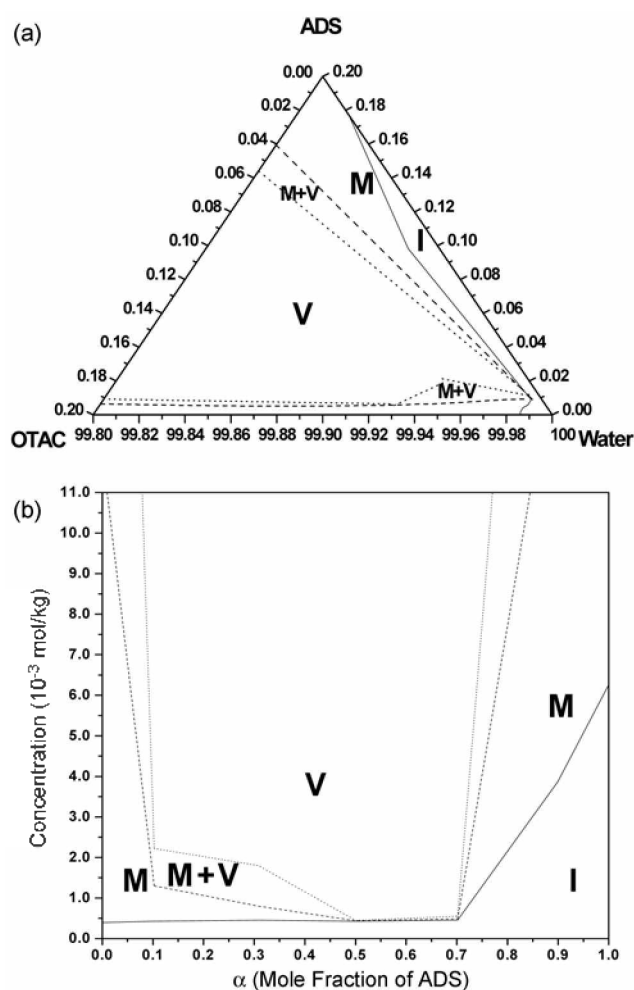


**Figure 2.** Phase behavior of very dilute aqueous mixtures of the anionic ADS and cationic OTAC (a) in a triangular coordinate and (b) in a rectangular coordinate. See the text for the symbols.

OTAC were formed. The mixed CMCs were measured by surface tensiometry and electrical conductometry, and the phase boundary between the isotropic and the micellar regions were determined by connecting these mixed CMCs.

In the region denoted as V, the mixture fluid was turbid and the turbidity appeared to increase with total surfactant concentration. At the fixed total surfactant concentration the turbidity increased with  $\alpha$ , the ratio of ADS moles to total mixed surfactant moles. In this region the existence of vesicles was confirmed by negative-staining transmission electron microscopy (TEM) and entrapment of a dye. With the equal amount of each surfactant (*i.e.*,  $\alpha = 0.5$ ), precipitates were observed, which are believed to be the catanionic surfactant complex  $\text{OTA}^-\text{DS}^-$ .

In the region denoted as M+V, the mixture fluid was tinted blue when the total surfactant concentration was less than about 2 m molal. It became turbid as the total surfactant concentration increased. In this region mixed micelles and vesicles coexisted, as evidenced by SANS. An observation unique to this region is that the region is so narrow for  $\alpha$  values between 0.5 and 0.7 that it appears to neighbor with the vesicular region at these  $\alpha$  values. Hence, micelles in the

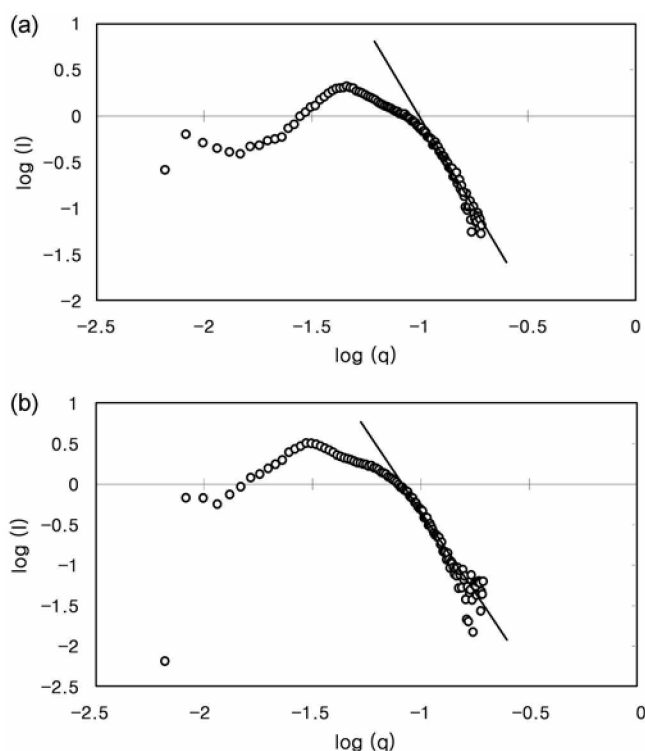


**Figure 3.** Plots of  $\log I$  vs.  $\log q$  of the SANS data for aqueous (a) 10 mM ADS and (b) 9 mM OTAC solutions. The slopes and the correlation coefficients are (a)  $-3.902$ ,  $0.9826$  and (b)  $-3.994$ ,  $0.9950$ , respectively.

M+V region (probably wormlike micelles as observed in another catanionic system of cetyltrimethylammonium-*p*-toluenesulfonate and sodium dodecylbenzenesulfonate)<sup>10</sup> might change to vesicles with addition of ADS (*i.e.*, with increase in  $\alpha$ ).

**Characterization of the Phase Regions.** *Region M:* The region M of Figure 2 was investigated by SANS. At  $\alpha = 0$  and  $\alpha = 1$ , *i.e.*, for pure-component micelles of OTAC and ADS, the SANS data (Figure 3) shows that the micelles are spherical according to the Porod law,<sup>35</sup> because the exponent in the plot of  $\log I$  vs.  $\log q$  is 4. The SANS intensity  $I$  is usually described by the power law  $I(q) \sim q^{-n}$  and the exponent  $n$  provides the information on the shapes of the surfactant association structures, as presented in Table 1. The power-law exponent  $n$  were determined as 3.902 and 3.994 for aqueous 10 mM ADS and 9 mM OTAC solutions. In determining  $n$ , the high- $q$  portions of the plots were used.<sup>36-38</sup>

The shape of the micelles observed by SANS is in agreement with that by geometric analysis. Geometrical packing properties of surfactant molecules are one of the important factors for the formation of association structures. It is usually expressed by the so-called critical packing parameter or surfactant number,  $N_p = v/a_0 l_c$ , where  $v$  is the volume of the hydrocarbon chain and is determined by

$$v = (27.4 + 26.9 n_c) \times 10^{-3} \text{ (nm}^3\text{)} \quad (1)$$

and  $l_c$  is an optimal length close to the fully extended

**Table 1.** The exponent  $n$  and the shape of the surfactant association structures

$n$	Shape	Remark
1	Cylinder or Rod	
2	Bilayer	
4	Sphere or Globule	Porod law <sup>35</sup>

hydrocarbon chain length  $l$ . The length  $l_c$  is determined by

$$l_c = 1 \times 0.77 = (0.154 + 0.1265n_c) \times 0.77 \text{ (nm)} \quad (2)$$

Here  $n_c$  is the carbon number of the alkyl chain of the surfactant and the factor 0.77 accounts for the fact that the alkyl chain is usually not fully extended. The validity of this factor was already discussed by Tanford.<sup>39</sup> Meanwhile, the head group area  $a_h$  of the surfactant is determined from the slope of surface tension versus concentration,  $\gamma$ - $\log C$ .<sup>40</sup>

When the surfactant molecules are conical, *i.e.*, when  $v/a_h l_c < 1/3$ , micelles are formed. In contrast, when they are cuplike, *i.e.*, when  $1/2 < v/a_h l_c < 1$  vesicles are formed.<sup>41</sup> For OTAC and ADS, the values of the critical packing parameter were determined as 0.2 and 0.37 from the  $\gamma$ - $\log C$  plots.<sup>42</sup> These values point to the fact that OTAC and ADS surfactants are likely to form spherical micelles in aqueous solutions, because  $N_p$  is less than or around  $1/3$ .<sup>41</sup>

Knowing that the micelles were spherical, their sizes were determined by the Guinier law,<sup>43</sup> which states that the intensity is described by  $I(q) = I(0)\exp[-(R_g/3)q^2]$  for which  $0.5 < qR_g < 1.4$  with  $R_g$  being the radius of gyration. Plots of  $\ln I$  vs.  $q^2$  yielded  $-R_g/3$  as the slope and the radius  $R$  was found from the  $R = \sqrt{5/3}R_g$ .<sup>44</sup> The radii of OTAC and ADS were determined as 30 and 20 Å (the diameters were 60 and 40 Å), respectively.

**Region M+V:** In this region the mixed surfactant samples appeared to be tinted blue at lower and turbid at higher total surfactant concentrations. This may indicate the coexistence of micelles and vesicles in this region; micelle-rich at lower and vesicle-rich at higher concentrations. In fact, SANS measurements support the coexistence of the micelles and vesicles in this region. Figure 4 shows the SANS data for the samples of 0.75 and 1.5 mM total surfactant concentrations at  $\alpha = 0.2$ . The  $n$  values in the  $\log I$  vs.  $\log q$  plots were 1.35 and 1.52, which correspond to the values between 1 for the cylinder and 2 for the bilayers. These results imply that cylindrical or rod micelles and vesicles coexist in this region.

**Region V:** Spontaneous vesicle formation was observed in the region denoted as V. The total surfactant concentration for which vesicles were observed was as low as 0.5 m molal and it depended on  $\alpha$ . Vesicle formation was confirmed by negative staining transmission electron microscopy (TEM) and by entrapment of bromophenol blue dye. Figure 5 shows negative staining TEM micrographs at  $\alpha = 0.7$  and 0.5, respectively. Vesicles and vesicle bilayers are clearly seen. Vesicles similar to those in Figure 5 were observed at all  $\alpha$  values except at  $\alpha = 0.5$ . At  $\alpha = 0.5$  cation/anion (or catanionic) mainly complexes were observed as precipitates with a few vesicles (Figure 5b). This finding is consistent

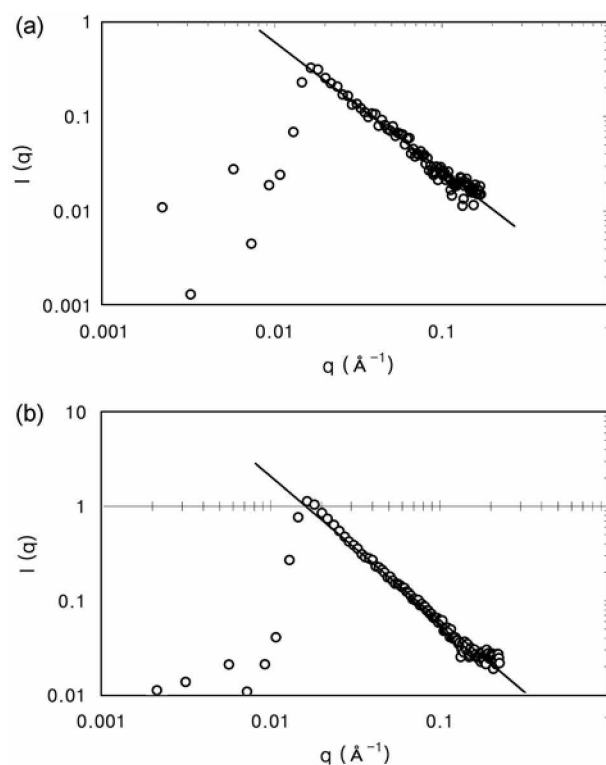


**Figure 4.** Plots of  $\log I$  vs.  $\log q$  of the SANS data for the mixed surfactant samples of the total surfactant concentrations of (a) 0.75 mM and (b) 1.5 mM at  $\alpha = 0.2$ .

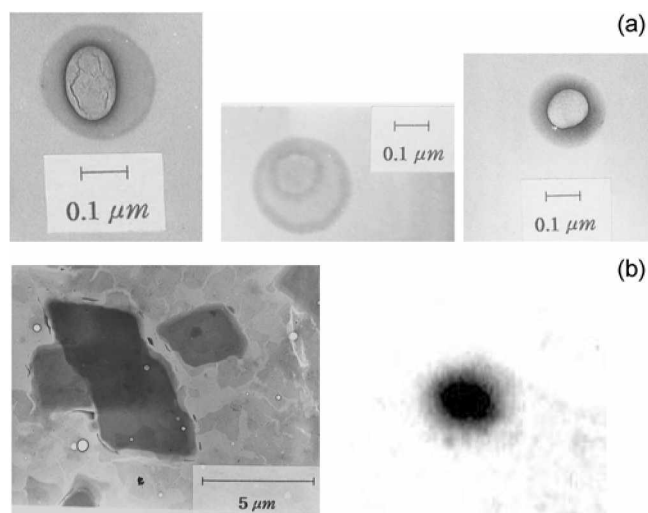


**Figure 5.** Negative staining TEM micrographs at (a)  $\alpha = 0.7$  and (b)  $\alpha = 0.5$ .

with the previous observations that the greatest amount of precipitation was observed at an equimolar mixture.<sup>17,45</sup> The complexes (OTA-DS), which are highly insoluble in water, might consist of octadecyltrimethyl cation (OTA<sup>+</sup>) and dodecyl sulfate anion (DS<sup>-</sup>). During the formation of the precipitates,  $\text{NH}_4\text{Cl}$  was produced and affected the pH of the mixture along with the unreacted monomer ions and counterions. The pH changed in the range of 4.5 and 6 and it decreased with the total surfactant concentration, irrespec-

**Table 2.** Values of  $v/a_0l_c$  at different mole ratios ( $\alpha$ 's) of ADS to OTAC

$\alpha$	$a_0$ (nm <sup>2</sup> )	$v/a_0l_c$
0.1	0.50	0.55
0.3	0.41	0.67
0.5	0.13	2.1
0.7	0.42	0.66

five of  $\alpha$ .

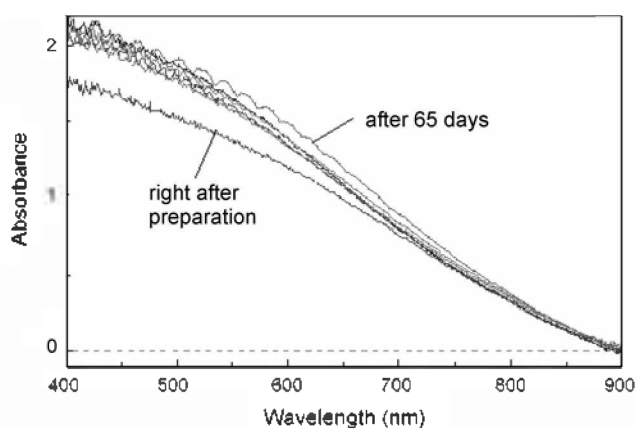
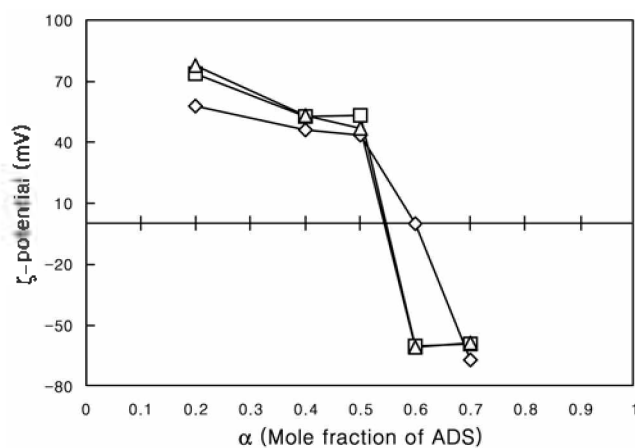
ADS and OTAC molecules are conical and they form spherical micelles in aqueous solutions of respective pure surfactants. However, when these surfactants are mixed in water, they are paired to result in the truncated conical shape. The critical packing parameter  $v/a_0l_c$  at various  $\alpha$ 's is calculated with  $a_0$  obtained by the surface tension data for the mixed surfactant samples.<sup>38,42</sup> Its value (Table 2) falls in  $1/2 < v/a_0l_c < 1$ , except at  $\alpha = 0.5$  for which precipitates were observed. The  $v/a_0l_c$  values support that cationic vesicles were formed at these  $\alpha$ 's.

The existence of vesicles was also checked by encapsulation of the bromophenol blue dye. The color change in the vesicle samples before and after gel filtration was obvious.<sup>42</sup> Encapsulation of dissolvable substance is one of the important functions of vesicles, and such encapsulation may make vesicles excellent drug delivery vehicle. The encapsulation efficiency ( $EF$ ) was calculated by  $EF = (C_{t,dye} - C_{un,dye})/C_{t,dye}$  where  $C_{t,dye}$  and  $C_{un,dye}$  are the total and uncaught dye concentrations, respectively.  $EF$  for the ADS/OTAC vesicles were measured as 17%, which was higher than  $EF$  for the sodium 10-undecenoate/DTAB vesicles reported in the literature.<sup>31</sup>

**Spontaneously Formed ADS/OTAC Vesicles. Stability of Vesicles:** UV absorbances of the vesicles right after their formation and after 4, 7, 10, 30, and 65 days were measured to examine the stability of the vesicles. Figure 6 shows the absorbance spectra at different days. The absorbances remained virtually unchanged for two months, implying that the vesicles exhibit long-term stability.

Zeta potentials of the vesicles were measured at different total concentrations and the results are presented in Figure 7. As  $\alpha$  increased,  $\zeta$  potential decreases and becomes negative between  $\alpha = 0.5$  and 0.6. For  $\alpha$  values smaller than 0.5,  $\zeta$  potentials are positive because the mixed systems are OTAC-rich, and ADS-poor. Generally it is thought that value of zeta-potential is zero at  $\alpha = 0.5$  since relative molarity of ADS and OTAC is identical. However, Figure 7 shows that the zero value of  $\zeta$  potential takes place around  $\alpha = 0.6$ . As  $\alpha$  increases, the system becomes ADS-rich and therefore the  $\zeta$  potentials become negative. The absolute values of  $\zeta$  potentials in the vesicle region are large in magnitude (40–70 mV). Hence, strong repulsive forces exist among vesicles and the long-term stability of the vesicles, which were manifested in the UV absorbance spectra, may be attributed to their high zeta potentials.

**Sizes of Vesicles:** The sizes of vesicle at  $\alpha = 0.7$  and various total different surfactant concentrations were measured

**Figure 6.** Changes in UV absorbance of ADS/OTAC vesicle samples at  $\alpha = 0.6$ .**Figure 7.** Zeta potentials of ADS/OTAC vesicles at various  $\alpha$  and total surfactant concentrations of 3 ( $\Delta$ ), 5 ( $\square$ ), and 10 ( $\circ$ ) mM.

using light scattering (Malvern Instruments Ltd, UK) and Laser Particle Analyzer (LPA-3000, Otsuka Electronics) and the results are presented in Figure 8. At lower surfactant concentrations two methods yielded almost identical vesicle sizes and at higher concentrations light scattering provided 20% larger sizes than laser particle analyzer. As the surfactant concentration increased, the vesicle size decreased; it decreased sharply up to 2 mM and then the rate of decrease was substantially reduced. The decrease in vesicle size with increasing surfactant concentration is in good agreement with an early study by Evans and Ninham<sup>46</sup> on didodecyl dimethyl ammonium hydroxide (DDAOH)/ water system.

**SANS Analysis of Vesicles:** Figure 9 shows the SANS data for the vesicle samples with the total surfactant concentrations of 4 mM at  $\alpha = 0.2$  and 5 and 8 mM at  $\alpha = 0.3$ . Over the entire range studied, the decay pattern in the plots of  $I(q)$  vs.  $q$  obeys the power law,  $I(q) \sim q^{-n}$ . The values of  $n$  are 2, 2.45 and 2.5. The decay patterns for these  $n$  values are compared to that of 2 (*i.e.*  $q^{-2}$ , solid line in Figure 8) which represents scattering from a bilayer structure.<sup>47</sup> The proximity of  $n$  to 2 supports that the colloidal particles formed were vesicles.

The SANS spectra of the vesicles at other  $\alpha$  values exhibit

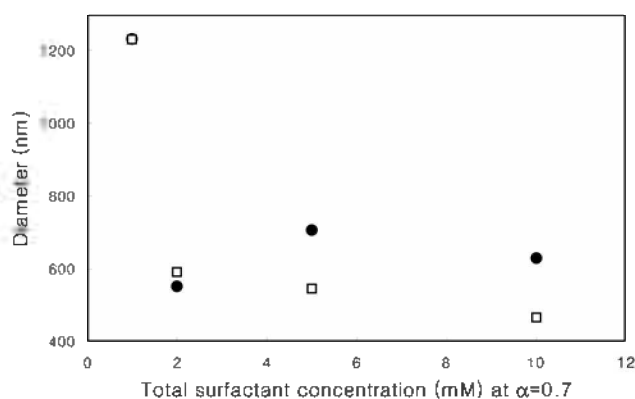


**Figure 8.** Sizes of ADS/OTAC vesicles measured by light scattering ( $\odot$ ) and laser particle analyzer ( $\square$ ) at  $\alpha = 0.7$  and various total surfactant concentrations.

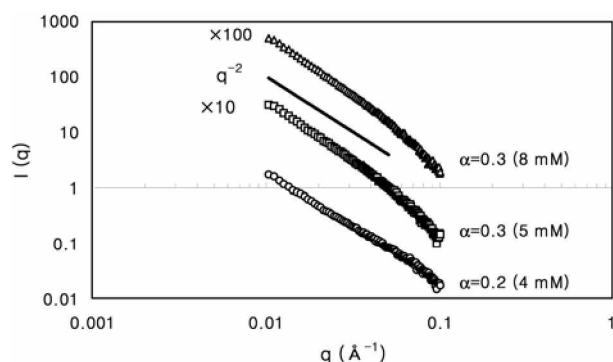


**Figure 9.** SANS data for the vesicle samples of 4 mM at  $\alpha = 0.2$ , and 5 and 8 mM at  $\alpha = 0.3$ .

similar behavior. Figure 9 shows the SANS data for  $\alpha = 0.7$ . The absolute values of the slopes (2.3 to 2.5) in the  $\ln I - \ln q$  plots are very close to 2, irrespective of total surfactant concentration. This result also manifests that the particles formed were vesicles.

The lamellar thickness ( $d_L$ ) of the vesicles can be obtained from the slope of Sheet Guinier plots,  $\ln[I(q)q^2]$  vs.  $q^2$ , of the SANS data.<sup>48</sup> Figure 10 shows such plots and the slopes (solid lines) at low  $q$  values. The thickness  $d_L$  was calculated from  $d_L/12 = \text{slope}$  and the results are presented in Table 3. As the total surfactant concentration increased, the lamellar thickness decreased. This may be responsible for the decrease in vesicle size with increasing surfactant concentration, which were manifested by light scattering and laser particle analyzer.

## Conclusions

The phase behavior of the ADS/OTAC/water system was investigated. When water is very rich and the total surfactant concentration is below 0.4 wt %, four distinct phase regions of isotropic molecular solution (I), micellar solution (M), vesicles (V), and a mixture of micelles and vesicles (M+V) have been observed. Each of the phase regions was examined by visual inspection, CMC measurements, transmission electron microscopy (TEM), small-angle neutron scattering

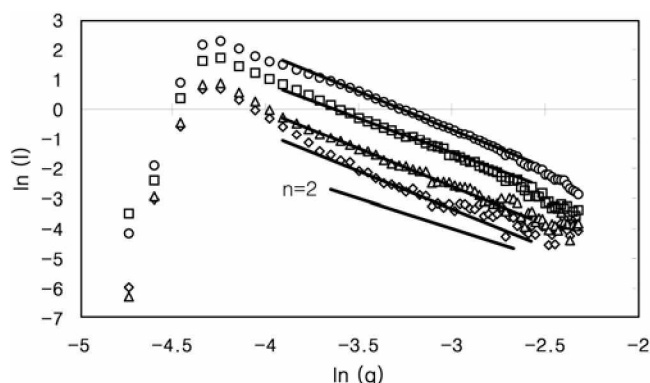


**Figure 10.** Plot of  $\log I$  vs.  $\log q$  for vesicle samples at  $\alpha = 0.7$  and total surfactant concentrations of 1 ( $\odot$ ), 2 ( $\triangle$ ), 5 ( $\square$ ), and 10 ( $\circ$ ) mM.

**Table 3.** The lamellar thickness as a function of total surfactant concentration for the vesicles at  $\alpha = 0.7$

Total surfactant concentration (mM)	$d_L$ (nm)
1	$15 \pm 2$
2	$12 \pm 2$
5	$9 \pm 1$
10	$5 \pm 1$

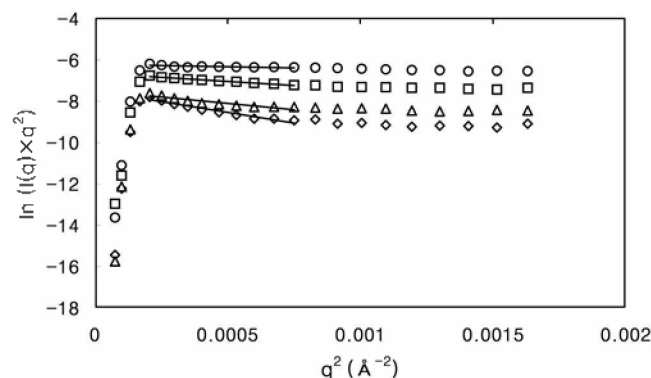


**Figure 11.** Sheet Guinier plots of SANS spectra for the vesicles at  $\alpha = 0.7$  and total surfactant concentrations of 1 ( $\odot$ ), 2 ( $\triangle$ ), 5 ( $\square$ ), and 10 ( $\circ$ ) mM.

(SANS), light scattering, and laser particle analyzer.

In the vesicular region, the ADS/OTAC mixed surfactant vesicles were formed spontaneously. Their existence was observed by TEM and their characteristics were examined by geometric analysis of critical packing parameter, encapsulation efficiency (EF), and SANS. The vesicle's EF of the bromophenol dye was 17%. The size of vesicles ranged from 450 nm to 120  $\mu\text{m}$  and it decreased with increasing total surfactant concentration. Such observation was also made with the didodecyl dimethyl ammonium hydroxide and water system.

The bilayer structure of the vesicles was confirmed by the power law  $I(q) \sim q^{-3}$  of the SANS spectra. The lamellar thickness of the vesicles was also determined from the spectra and it decreased from 15 to 5 nm with increasing total surfactant concentration. This result may be responsible

for the decrease in vesicle size with increasing surfactant concentration.

The vesicles exhibited long-term stability, as UV absorbance spectra remained almost same for two months. Zeta potentials of the vesicles were large in magnitude (40-70 mV) and the observed long-term stability of the vesicles may be attributed to such high  $\zeta$  potentials.

**Acknowledgements.** This work was partially supported by the Korea Science and Engineering Foundation grant (R01-2001-00308) and Chung-Ang University Instrument grant. H.-U. Kim was supported by the Korea Research Foundation (Program No.: EN0037). The authors are also grateful to Drs. B. S. Sung and Y. S. Han at the Korea Atomic Energy Research Institute for their assistance with SANS experiment.

### References

- Holland, P. M.; Roubingh, D. N. *Mixed Surfactant Systems*. Am. Chem. Soc.: Washington, DC, 1992.
- Ogino, K.; Abe, M. *Mixed Surfactant Systems*. Marcel Dekker: New York, 1993.
- Lucassen-Reynders, E. H.; Lucassen, J.; Giles, D. *J. Colloid Interface Sci.* **1989**, *81*, 150.
- Yu, Z. J.; Zhao, G. X. *J. Colloid Interface Sci.* **1989**, *130*, 414.
- Kaler, E. W.; Murthy, A. K.; Rodriguez, B. E.; Zasadzinski, J. A. *Science* **1989**, *245*, 1371.
- Uchegbu, I. F.; Vyas, S. P. *Int. J. Pharm.* **1998**, *172*, 33.
- Fendler, J. H. *Membrane Mimetic Approach to Advanced Materials*. Springer-Verlag: Berlin, 1992.
- Yu, W. L.; Pei, J.; Huang, W.; Zhao, G. X. *Mater. Chem. Phys.* **1997**, *49*, 87.
- Yaacob, I. I.; Nunes, A. C.; Bose, A. *J. Colloid Interface Sci.* **1995**, *171*, 73.
- Kaler, E. W.; Herrington, K. L.; Murthy, K. A.; Zasadzinski, J. A. *J. Phys. Chem.* **1992**, *89*, 6698.
- Chiruvolu, S.; Istraclachvili, J. N.; Naranjo, E.; Xu, Z.; Zasadzinski, J. A. *Langmuir* **1995**, *11*, 4256.
- Herrington, K. L.; Kaler, E. W.; Miller, D. D.; Zasadzinski, J. A.; Chiruvolu, S. *J. Phys. Chem.* **1993**, *97*, 13792.
- Bergstrom, M.; Pedersen, J. S. *Langmuir* **1998**, *14*, 3754.
- Blankschein, D.; Yuet, P. K. *Langmuir* **1996**, *12*, 3819.
- Yateilla, M. T.; Herrington, K. L.; Brasher, L. L.; Kaler, E. W.; Chiruvolu, S.; Zasadzinski, J. A. *J. Phys. Chem.* **1996**, *100*, 5874.
- Marques, E.; Khan, A.; da Gracia Miguel, M.; Lindmann, B. *J. Phys. Chem.* **1993**, *97*, 4729.
- Kondo, Y.; Uchiyama, H.; Yoshino, N.; Nishiyama, K.; Abe, M. *Langmuir* **1995**, *11*, 2380.
- Allardice, A.; Gummo, G. *Cosmetics and Toiletries* **1988**, *103*, 107.
- Jurezyk, M. F.; Berger, D. R.; Damaso, G. R. *Cosmetics and Toiletries* **1991**, *106*, 63.
- Kekicheff, P.; Grabielle-Madellmont, C.; Ollivon, M. *J. Colloid Interface Sci.* **1989**, *131*, 112.
- Kekicheff, P. *J. Colloid Interface Sci.* **1989**, *131*, 133.
- Kurz, J. L. *J. Phys. Chem.* **1962**, *66*, 2239.
- Muramatsu, C.; Inoue, M. *J. Colloid Interface Sci.* **1976**, *55*, 80.
- Rosen, M. J. *Surfactants and Interfacial Phenomena*, 2nd ed.; John Wiley & Sons: New York, 1989; pp 14-15.
- Porter, M. R. *Handbook of Surfactants*; Chapman and Hall: New York, 1991; pp 70-73.
- Fox, C. *Cosmetics and Toiletries* **1988**, *103*, 25.
- Hunting, A. L. *Encyclopedia of Shampoo Ingredients*. Micelle Press: London, 1983.
- Kang, K.-H.; Kim, H.-U.; Lim, K.-H.; Jeong, N.-H. *Bull. Korean Chem. Soc.* **2001**, *22*, 1009.
- Armarego, W. L. F.; Perrin, D. D. *Purification of Laboratory Chemicals*, 4th ed.; Butterworth Heinemann: Singapore, 1996.
- Kunitake, T.; Okahata, U. *J. Am. Chem. Soc.* **1980**, *102*, 549.
- Zhao, G.-X.; Yu, W.-L. *J. Colloid Interface Sci.* **1995**, *173*, 159.
- Pedersen, J. S.; Egelhaaf, S. U.; Schurtenberger, P. *J. Phys. Chem.* **1995**, *99*, 1299.
- Laughlin, R. G. *The Aqueous Phase Behavior of Surfactants*. Academic Press: London, 1994; p 472.
- Kang, K.-H.; Kim, H.-U.; Lim, K.-H. *Colloid Surf. A* **2001**, *189*, 113.
- Porod, G. In *Small-Angle X-ray Scattering*; Glatter, O.; Kratky, O., Eds.; Academic Press: New York, 1982; p 17.
- Debye, P. *J. Phys. Chem.* **1947**, *51*, 18.
- Debye, P. *J. Phys. Chem.* **1949**, *53*, 1.
- Roe, R.-J. *Methods of X-ray and Neutron Scattering in Polymer Science*. Oxford University Press: New York, 2000; pp 155-209.
- Tanford, C. *J. Phys. Chem.* **1974**, *78*, 2469.
- Evans, D. F.; Wennerstrom, H. *Colloidal Domain: Where Physics, Chemistry, Biology, and Technology Meet*, VCH Publishers Inc.: 1994; pp 68-69.
- Istraclachvili, J. N. *Intermolecular and Surface Forces*, 2nd ed.; Academic Press: San Diego, 1992; p 381.
- Kim, H.-U. Ph. D. Dissertation, Chung-Ang University, Seoul, 2002.
- Guinier, A.; Fournet, G. *Small-Angle Scattering of X-Ray*, John Wiley & Sons: New York, 1955.
- Feigin, L. A.; Svergun, D. I. In *Structure Analysis by Small-Angle X-Ray and Neutron Scattering*; Talyor G. W., Ed.; Plenum Press: London, 1987; pp 68-69.
- Salkar, R. A.; Mukesh, D.; Samant, S. D.; Manohar, C. *Langmuir* **1998**, *14*, 3778.
- Evans, D. F.; Ninham, B. W. *J. Phys. Chem.* **1986**, *90*, 226.
- Iampietro, D. J.; Kaler, E. W. *Langmuir* **1999**, *15*, 8590.
- Ma, G.; Barlow, D. J.; Lawrence, M. J.; Heenan, R. K.; Timmins, P. *J. Phys. Chem. B* **2000**, *104*, 9081.